2021 43rd Annual International Conference of the
IEEE Engineering in Medicine & Biology Society (EMBC)
Oct 31 - Nov 4, 2021. Virtual Conference

Decoding Human Cognitive Control Using Functional Connectivity of Local Field Potentials

Sandeep Avvaru, *Student Member*, *IEEE*, Nicole R. Provenza, Alik S. Widge, and Keshab K. Parhi, *Fellow*, *IEEE*

Abstract— **Many patients with mental illnesses characterized by impaired cognitive control have no relief from gold-standard clinical treatments resulting in a pressing need for new alternatives. This paper develops a neural decoder to detect task engagement in ten human subjects during a conflict-based behavioral task known as the multi-source interference task (MSIT). Task engagement is of particular interest here because closed-loop brain stimulation during those states can augment decision-making. The functional connectivity patterns of the electrodes are extracted. A principal component analysis of these patterns is carried out and the ranked principal components are used as inputs to train subject-specific linear support vector machine classifiers. In this paper, we show that task engagement can be differentiated from background brain activity with a median accuracy of 89.7%. This was accomplished by constructing distributed functional networks from local field potentials recording during the task performance. A further challenge is that goal-directed efforts take place over higher temporal resolution. Task engagement must thus be detected at a similar rate for proactive intervention. We show that our algorithms can detect task engagement from neural recordings in less than 2 seconds; this can be further improved using an application-specific device.**

I. Introduction

Neuropsychiatric disorders are the leading cause of disability in the United States; about one in every five American adults experiences mental illness. Existing treatments for mental illness are less than 50% effective, which leaves many patients with behavioral disorders with degraded well-being [1]. The ineffectiveness of existing treatments is partly due to a lack of mechanistic understanding of the disorders and the consequent inability to address the cognitive symptoms. Dysfunctional cognitive control characterizes a wide range of mental disorders such as depression, addiction, anxiety disorders, autism spectrum disorders, and schizophrenia [2]–[6]. Therefore, there is a pressing need to study the neurological mechanisms underlying these disorders and develop new ways to rectify impaired cognitive control. Effective cognitive control involves restricting and controlling default responses in favor of a more desired adaptive response.

Electrical deep brain stimulation (DBS) has shown some promise in modulating the brain circuits underlying abnormal behaviors. It has been proposed as a more effective approach for treating mental illnesses such as Parkinson's disorder, major depressive disorder (MDD), and obsessive-compulsive disorder (OCD) [7]–[9]. However, it suffers from ambiguous clinical outcomes, which limits its usage [8]. Therefore, further research is required to understand its mechanisms of action fully. Additionally, the optimal parameters of stimulation are still unknown. Increasing evidence suggests that adapting DBS parameters to a desired psychological effect, commonly known as *closed-loop DBS*, can be helpful [10]–[12]. Since stimulation during healthy activity can interfere with normal function, it is critical to identify mental states of cognitive effort (e.g., decision making during a task) to target for intervention. However, there is no established signature for engagement in mentally demanding tasks.

This paper decodes local field potential (LFP) signals recorded from ten participants performing the multi-source interference task. The goal is to differentiate task engagement from background mental activity. Brain connectivity can be used to discover biomarkers that distinguish psychiatric disorders [13]–[15]. To this end, LFP based functional networks were utilized. Reliable detection of task-engagement can provide objective biomarkers to trigger stimulation. Thus, it could facilitate the development of closed-loop neuromodulation to prospectively bias a decision-making process before it begins. A prior study showed that task and rest states could be separated [16]. However, we found that the analysis in [16] suffers from a few drawbacks. The algorithm suffers from data-leakage, which results in an unreliable evaluation of the classifiers. More specifically, (1) the feature extraction utilizes test data that should be independent of the training data, and (2) the training and test data were not temporally separated. This paper outperforms the previous approach by identifying task engagement with 89.7% median classification accuracy.

The rest of the paper is organized as follows. Section II describes the task, data and methods. Section III presents the

The data were originally collected with support from the Defense Advanced Research Projects Agency (DARPA) under Cooperative Agreement Number W911NF-14-2-0045 issued by ARO contracting office in support of DARPA's SUBNETS Program. S. Avvaru was supported by the MNDrive Neuromodulation Research Fellowship. A.S. Widge acknowledges additional research support from the MNDrive Brain Conditions program, the UMN Medical Discovery Team on Addiction, and the National Institutes of Health (R01NS113804, R01MH123634). All views presented herein are those of the authors, not the policy of any government agency or other funding body.

This research was supported in part by the National Science Foundation under grant number CCF-1954749.

S. Avvaru and K. K. Parhi are with the Department of Electrical and Computer Engineering, University of Minnesota, Minneapolis, MN 55455, USA (email: avvar002@umn.edu and parhi@umn.edu).

N. R. Provenza is with Brown University School of Engineering, Providence, RI, USA

A. S. Widge is with the Department of Psychiatry and Behavioral Sciences, University of Minnesota, Minneapolis, MN 55455, USA

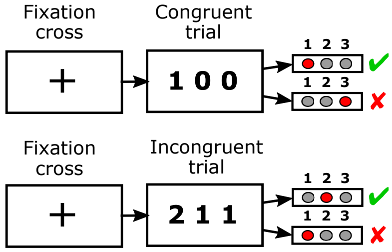

(a) Examples of congruent and incongruent trials

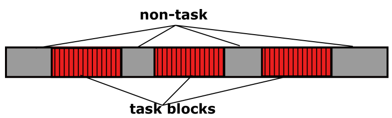

(b) Block structure of the MSIT trials

Fig. 1: The Multi-Source Interference Task (MSIT).

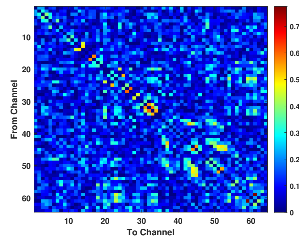

(a) Task

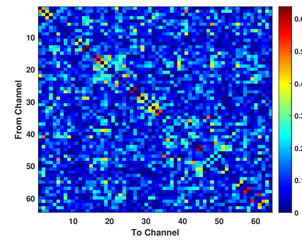

(b) Non-Task

Fig. 2: Functional network of a randomly chosen task and non-task segments from one subject constructed using local field potential signals from 64 channels.

results. Section IV concludes the paper.

II. Materials and Methods

A. The Multi-Source Interference Task (MSIT)

The multi-source interference task is a well-established paradigm that involves multiple dimensions of cognition, including but not limited to attention, object recognition, and decision making, and is a useful tool to study the network basis of cognition [17]. Its sensitivity to electrical stimulation makes it a good candidate task to study cognitive control [11], [18]. In an MSIT trial (see Fig. 1), the participants are presented with a fixation cross for 2 seconds followed by a stimulus in the form of 3 digits – one of which is the 'target.' Two of the three numbers, known as 'distractors,' have the same value. The target is either 1, 2, or 3. The experiment includes 'congruent' and 'incongruent' trials. In the congruent condition, the distractors are always '0', and the target's position matches its value. In the incongruent (also known as interference) condition, the distractors are picked from potential targets, and the position of the unique target is different from its keyboard position (Simon effect). In a successful trial, the participant reports, via a button press on a keypad, the target's value regardless of its position. Examples of congruent and incongruent trials are presented in Fig. 1(a).

The experiment consists of up to 5 blocks of trials, with approximately 32 or 64 trials in each block (Fig. 1(b)). Signals recorded between the blocks, before the first block, and after the last block were labeled as non-task data. The task contained a roughly equal number of congruent and incongruent trials. Median success rates of $100\% \pm 2.47\%$ and $97.1 \pm 5.52\%$ were reported during congruent and incongruent conditions, respectively [16].

B. Data Description

The experiment included ten voluntary participants with long-standing epilepsy who performed the task while hospitalized. All procedures were approved by the local institutional review boards at the Partners Healthcare (Massachusetts General Hospital) and the US Army Human Research Protection Office. Depth electrodes with diameters varying between 0.8 mm and 1 mm were implanted for epilepsy monitoring. Local field potentials were recorded utilizing these depth electrodes during the task and rest periods with free behavior. The signals were referenced to a scalp EEG electrode. Each electrode had 8–16 platinum/iridium contacts that measured LFP signals at a 2 kHz sampling rate. There were at least five such electrodes (maximum of nine) in each hemisphere. Channels with excessive line noise or other visually noticeable artifacts were eliminated. Line noise and its harmonics were removed via filtering in the remaining channels. The EEG signals were also bipolar re-referenced for the analysis. Further details about the data can be found in [16].

C. Class Label Assignment

The neural activity recorded during MSIT trials is referred to as *task data*, and the data recorded during rest periods (before or after trial blocks) is referred to as *non-task data*. To differentiate between the task and non-task states, the signals were divided into multiple task segments and non-task segments. The time when the fixation cross was presented during a trial was marked as the trial's start. The time duration between two consecutive fixation crosses determined the length of each trial. The duration of trials varies depending on the subjects' reaction times. 3.8-second (minimum trial duration for most subjects) time segments from every trial's start were labeled 'task' data. The signals recorded during rest periods were windowed into 'non-task' segments with a window length equal to the minimum task duration. Overlapping windows were used when the number of non-task segments was less than the number of task segments. If the amount of task data was less than the amount of non-task data, only a subset of the non-task data was used for classification. Thus, the two classes were balanced to make sure the classifiers are not biased.

D. Feature Extraction

Functional networks were then constructed for each task/non-task segment by computing its correlation matrix. Fig. 2 depicts examples of the task and non-task functional networks in the form of adjacency matrices. Each

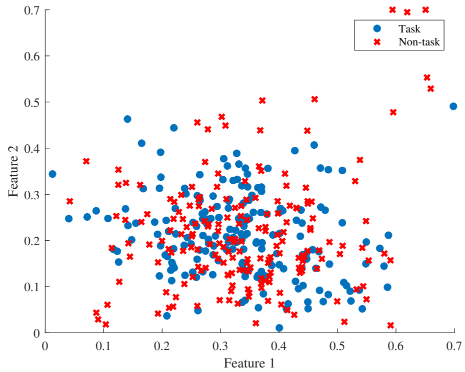

(a) Edge Strengths

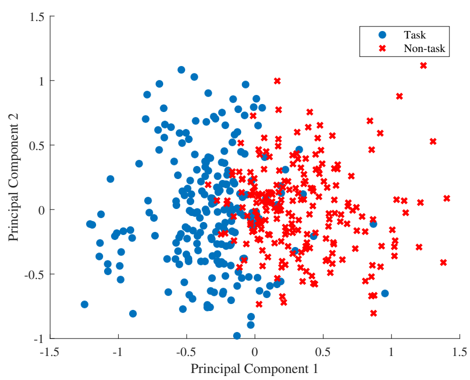

(b) First two principal components

Fig. 3: Two-dimensional scatter plot of two features before and after PCA from task and non-task data of subject-1.

entry in an adjacency matrix represents the strength of the connection (also known as the edge strength) between the two channels given by its row and column numbers. The adjacency matrices are symmetric matrices indicating that they are undirected correlational networks. The diagonals were set to zeros for better visualization. To extract useful patterns in these networks and eliminate redundancy, we employ *principal component analysis* (PCA). PCA is a dimensionality reduction method that attempts to reduce the number of variables while preserving as much information as possible. The resultant principal components are unique linear combinations of the edge strengths such that their variance is maximized. Maximizing the variance aids in differentiating between the two states: task and non-task. The PCA coefficients were computed only using the training data to ensure no information leakage into the test data.

III. Results

A. PCA Features

Functional networks shown in Fig. 2 contain task-specific patterns of brain activity. A timeseries with N channels represents a network with N nodes, and $\binom{N}{2}$ connections. For example, a 64-channel recording would create 2016 features. The high dimensionality of the data makes it challenging to identify the patterns. PCA transforms the feature space such that the variance of the projections (in the new space) is maximized. The resultant features are usually more separable, aiding the classification process. Fig. 3(a) illustrates that when edge strengths are used as features, the two classes are not easily separable. In Fig. 3(b), we present a two-dimensional scatter plot of the first two principal components of subject-1. It can be observed that the task and non-task data are separable in the resultant feature space. Thus, PCA helps in finding patterns that differentiate task and non-task functional networks.

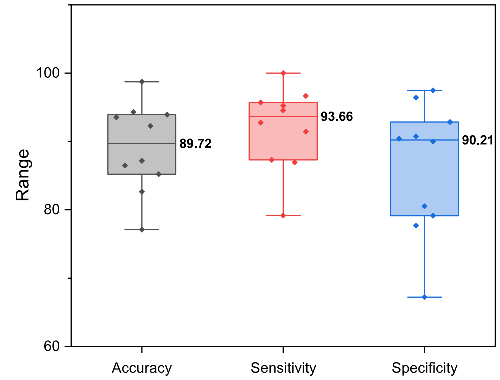

Fig. 4: Accuracy, sensitivity and specificity of task vs. non-task classification.

B. Classification Results

For each subject, the data were split into ten subsets via sequential sub-sampling to ensure that test samples are not in the training samples' temporal vicinity. One of the ten folds acts as the test set in each iteration, while the other nine act as the training data. This procedure, known as ten-fold cross-validation, ensures that all the data are tested and makes the classifiers less prone to overfitting. The PCA features were used as inputs to linear support vector machine (SVM) classifiers. The mean classification accuracy of the ten test sets was recorded. This process was repeated by changing the number of features/inputs from 1 to 150. The features with the highest cross-validation accuracy are considered the optimal features. Results of the classification for all subjects are presented in Table I. The median task vs. non-task prediction accuracy is $89.7 \pm 6.5\%$. This is a significant improvement over the $78.1 \pm 7.39\%$ reported in [16]. The task and non-task accuracies are $93.7 \pm 6.05\%$ and $90.2 \pm 9.69\%$, respectively. The summary of prediction accuracies is presented in Fig. 4.

C. Classifier Runtimes

Table I shows that the number of channels and, consequently, the number of optimal features, i.e., principal components (PCs), varies among the subjects. The computational complexity of the decoders is relatively low due to the simplicity of the approach. We computed the time taken to process a randomly chosen LFP segment, extract the features and determine its classifier outcome for each subject. These classifiers can be used to detect the task engagement in

TABLE I: Accuracy of task vs. non-task classifiers for the ten subjects. Sensitivity and specificity represent the task and non-task accuracies, respectively. Random label-assignment would result in a baseline accuracy of 50%.

Sub.	Num. ch.	Acc.	Sens.	Spec.	Num. of PCs
1	64	87.17	95.22	79.13	36
2	150	92.27	94.55	90.00	92
3	141	86.49	92.78	80.53	113
4	162	98.75	100.00	97.50	14
5	189	85.20	79.17	90.77	13
6	183	94.29	95.71	92.86	53
7	130	77.08	86.94	67.22	115
8	194	93.93	91.43	96.43	73
9	195	93.54	96.67	90.42	108
10	126	82.63	87.32	77.69	149

TABLE II: The time taken to predict whether the participant is engaged in the MSIT or not. Each column shows the mean and standard deviation of 100 runs of the algorithm on a 3.8 second multidimensional segment

Subject	1	2	3	4	5	6	7	8	9	10
μ(sec.)	2.09	1.99	2.04	1.57	1.65	1.88	1.89	1.42	1.55	1.50
σ(sec.)	0.09	0.15	0.07	0.09	0.13	0.18	0.09	0.03	0.11	0.04

2 seconds or less, as illustrated in Table II. The runtimes were calculated using MATLAB programs implemented on a general-purpose machine with an Intel Core i7-8565U processor and 16 GB memory.

IV. Discussion and Conclusion

Cognitive control refers to the effortful deployment of cognitive resources for adaptive response to the environment. Intact cognition consists of interrelated executive functions, including updating (i.e., monitoring working memory), inhibition (resisting prepotent responses), and shifting (switching between mental states) [19]. There is no well-defined neural signature for the mental effort associated with these coordinated cognitive processes that facilitate decision-making. Several studies show that cognitive control deficits are central symptoms in many psychopathological conditions, including schizophrenia, depression, and addiction. Interventions such as DBS that target the cognitive control networks could be influential for mitigating symptomatic distress, functional impairments, and diminished quality of life prevalent across psychiatric disorders. Developing effective therapeutics through adaptive neuromodulation requires rapid detection of focused mental activity.

This paper demonstrates that such mental states are encoded in the functional connectivity of the brain. Fig. 3 illustrates that neural correlates of task-related mental effort can be separated from background activity. The results in Fig. 4 and Table I show that task engagement can be detected with high accuracy. The proposed approach attains a median accuracy of 89.7%, a substantial increase from the 78.1% reported in [16]. There is some variation between the subjects, partly due to variation in the electrode implant setups; the number of channels varied between 64 and 195. Moreover, the non-task data involved recordings during free-behavior without any restrictions or standardization between the participants. This heterogeneity in the non-task activity might explain why the classifiers have slightly higher sensitivity than specificity. A limitation of the current work is that it is limited to a single task. The future work will be focused on applying the algorithm to multiple cognitive tasks.

References

[1] L. Shi, J. Sun *et al.*, "Brain networks of happiness: dynamic functional connectivity among the default, cognitive and salience networks relates to subjective well-being," *Social Cognitive and Affective Neuroscience*, vol. 13, no. 8, pp. 851–862, 08 2018.

[2] A. F. Arnsten and K. Rubia, "Neurobiological circuits regulating attention, cognitive control, motivation, and emotion: Disruptions in neurodevelopmental psychiatric disorders," *J. of the American Academy of Child & Adolescent Psychiatry*, vol. 51, no. 4, pp. 356 – 367, 2012.

[3] L. M. McTeague, J. Huemer *et al.*, "Identification of common neural circuit disruptions in cognitive control across psychiatric disorders," *American Journal of Psychiatry*, vol. 174, no. 7, pp. 676–685, 2017.

[4] N. Ma, Y. Liu *et al.*, "Addiction related alteration in resting-state brain connectivity," *NeuroImage*, vol. 49, no. 1, pp. 738 – 744, 2010.

[5] J. T. Nigg, G. M. Knottnerus *et al.*, "Low blood lead levels associated with clinically diagnosed attention-deficit/hyperactivity disorder and mediated by weak cognitive control," *Biological Psychiatry*, vol. 63, no. 3, pp. 325 – 331, 2008, impulse Control: Aggression, Addiction, and Attention Deficits.

[6] C. L. Fales, D. M. Barch *et al.*, "Altered emotional interference processing in affective and cognitive-control brain circuitry in major depression," *Biological Psychiatry*, vol. 63, no. 4, pp. 377 – 384, 2008, stress, Depression, and Circuitry.

[7] J. Massano and C. Garrett, "Deep brain stimulation and cognitive decline in parkinson's disease: A clinical review," *Frontiers in Neurology*, vol. 3, p. 66, 2012.

[8] A. S. Widge, D. A. Malone *et al.*, "Closing the loop on deep brain stimulation for treatment-resistant depression," *Frontiers in Neuroscience*, vol. 12, p. 175, 2018.

[9] A. Widge and D. Dougherty, "Deep brain stimulation for treatment-refractory mood and obsessive-compulsive disorders," *Current Behavioral Neuroscience Reports*, vol. 2, 08 2015.

[10] A. S. Widge, K. K. Ellard *et al.*, "Treating refractory mental illness with closed-loop brain stimulation: Progress towards a patient-specific transdiagnostic approach," *Experimental Neurology*, vol. 287, pp. 461 – 472, 2017.

[11] I. Basu, A. Yousefi *et al.*, "Closed loop enhancement and neural decoding of human cognitive control," *bioRxiv*, 2020.

[12] N. Provenza, E. Matteson *et al.*, "The case for adaptive neuromodulation to treat severe intractable mental disorders," *Frontiers in Neuroscience*, vol. 13, 02 2019.

[13] S. H. Chu, C. Lenglet *et al.*, "Classifying treated vs. untreated MDD adolescents from anatomical connectivity using nonlinear SVM," in *2018 40th Annual International Conference of the IEEE Engineering in Medicine and Biology Society (EMBC)*, 2018, pp. 1–4.

[14] B. Sen, G. A. Bernstein *et al.*, "Sub-graph entropy based network approaches for classifying adolescent obsessive-compulsive disorder from resting-state functional MRI," *NeuroImage: Clinical*, vol. 26, p. 102208, 2020.

[15] T. Xu, K. R. Cullen *et al.*, "Network analysis of functional brain connectivity in borderline personality disorder using resting-state fMRI," *NeuroImage: Clinical*, vol. 11, pp. 302–315, 2016.

[16] N. Provenza, A. Paulk *et al.*, "Decoding task engagement from distributed network electrophysiology in humans," *Journal of Neural Engineering*, vol. 16, p. 056015, 08 2019.

[17] G. Bush, L. Shin *et al.*, "The multi-source interference task: Validation study with fMRI in individual subjects," *Molecular psychiatry*, vol. 8, pp. 60–70, 01 2003.

[18] A. Widge, S. Zorowitz *et al.*, "Deep brain stimulation of the internal capsule enhances human cognitive control and prefrontal cortex function," *Nature Communications*, vol. 10, p. 1536, 04 2019.

[19] G. Gratton, P. Cooper *et al.*, "Dynamics of cognitive control: Theoretical bases, paradigms, and a view for the future," *Psychophysiology*, vol. 55, no. 3, p. e13016, 2018.